N72-21006

NASA TECHNICAL TRANSLATION NASA TT F-14,235

STABILITY AND CONTROL OF HYPERSONIC AIRCRAFT

R. Ceresuela

CASE FILE COPY

Translation of: "Stabilité et contrôle d'avions hypersoniques", Office National d'Etudes et de Recherches Aerospatiales, Report T.P. No. 1014, 1971. Also: l'Aeronautique et l'Astronautique, No. 29, 1971-5, pp. 33-47.

NATIONAL AERONAUTICS AND SPACE ADMINISTRATION
WASHINGTON, D.C. 20546 APRIL 1972

STABILITY AND CONTROL OF HYPERSONIC AIRCRAFT

René Ceresuela(1)

ABSTRACT. ONERA has undertaken a wind tunnel study up to speeds of Mach 5 and 7 of the influence of different engine types on pitch and roll stability. Compatibility of internal and external flows is examined for highly deformed intakes and exhausts.

Introduction /33*

The object of this report is to present several problems in the aerodynamics of sustained hypersonic flight, illustrated when possible by experimental results.

We shall first discuss the problem of maximal lift/drag ratio, then that of longitudinal and lateral stabilities related to large volume engines. We shall finally look at special aerodynamic difficulties which could be caused by the deformation of light and hot structures.

Aerodynamic Lift/Drag Ratio

It has been demonstrated that a hypersonic aircraft project is extremely /34
sensitive to different parameters — such as the structural efficiency or the propulsion efficiency, and the attainable aerodynamic lift/drag ratio. In

---

(1)Report presented at the International Council of the Aeronautical Sciences (ICAS, Rome, September, 1970). The figures are the original figures, with English wording.

*Numbers in the margin indicate the pagination in the original foreign text.

numerous parametric studies appearing in the last few years, the values adopted for this lift/drag ratio vary enormously from one author to another, because of a lack of published experimental results.

For example, Figure 1 compares the maximal lift/drag ratios considered by Ferri[1] and by Heldenfiels [2] in general studies, and the experimental values obtained at ONERA on a highly simplified shape with a very thin wing profile (NACA 64 A 002.5), without control surfaces, fins, and engines. The measured values are significantly less than prior estimates; one could expect the difference to be smaller for the complete aircraft shape.

In present supersonic transport projects, the lift/drag ratios achieved on sophisticated shapes are greater than those of the shapes initially considered. Improvements have been obtained, as is well-known, by elaborate longitudinal curvatures, accompanied by twisting and conical camber of the forward sections of delta wings, and by a general design conforming to the area law. It is also known that these improvements seek to optimize the shape at the cruising Mach number, but give little or no help at other flight velocities.

For the Mach-3 XB-70, the concept of favorable interaction was applied to the fullest, called "wave-riding", in which the shock wave of the immense engine nacelle gives an increase in lift by its action on the wing, while a part of the wave drag is cancelled. But it has been shown that this arrangement, recently recommended by Eggers from linear-theory considerations, does not result in a great advantage at high velocities. Figure 2 is taken from a report of tests at Langley by Becker [3]. It is clear that, at Mach numbers above 3, an increasing difference appears between predictions of linear calculations and the measured values, and that beyond Mach 7, the flat-bottom (FB) configurations are more efficient.

To show the maximum lift/drag ratios which could be hoped for at high Mach numbers, another series of measurements at $M = 6.8$ was collected by

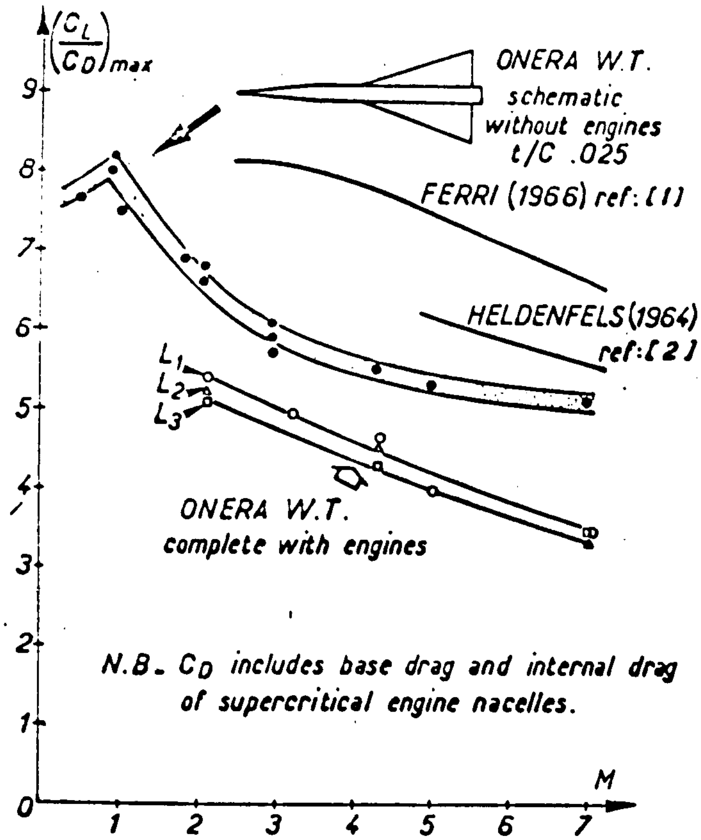

Figure 1. Aerodynamic lift/drag ratio of hypersonic aircraft.

Becker [3] on rectangular, delta, or "caret" wings, all with simple wedge profiles. These are the lower curves of Figure 2. The maximum lift/ drag ratios are shown as a function of the single accommodation parameter $V^{2/3}S^{-1}$. These data, combined with the difficulty of using the wing volume as a cryogenic reservoir, give little hope for notable gains in lift/drag ratio for hypersonic flight. /35

Structural research carried out since 1965, notably at Langley, has, however, led to the study of integrated shapes, where the wing and fuselage functions are no longer separate, with the goal of better volume efficiency. A first step in this direction is represented by the drawing of Figure 3, showing the HT 4 shape studied at Langley. Although the transverse sections are highly evolutional, one can still recognize the presence of separate relatively thin wings with rather pointed leading edges.

An even more radical design, the lower photograph of Figure 4, has been proposed by the Ames Center.

The general shape [4] where the plan view is a pure delta, is defined by an elliptical section at about 2/3 the length. The forward part is a

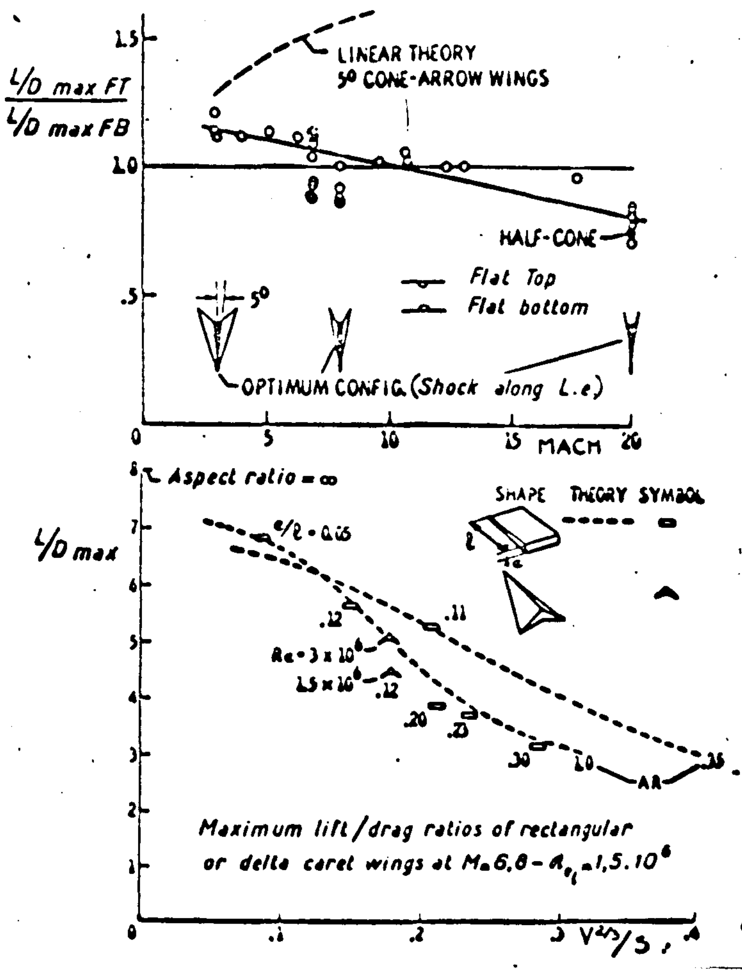

Figure 2. Lift/drag ratio compared for configurations with high and low wings at variable Mach numbers; effect of the volume parameter at M = 6.8.

conical surface resting on this ellipse; likewise, the after part is a conoid resting on the ellipse and on the rectangular pointed trailing edge.

The aerodynamic results obtained on these two shapes have not been published. It has been indicated, however [5], that the suppression of wings of the second shape reduces the structural weight with a modest loss of lift/drag ratio. Calculations of payload sensitivity for this project (Figure 5) taken from [6] show that a 1% reduction in structural weight compensates for a 2.5% loss in aerodynamic lift/drag ratio.

It may be expected that this second shape, the definition of which leads to variable radii along the leading edge, will be optimized for heating with difficulty, and that the flow over the bottom surface, which is irregular for the same reason, will present problems in the adaptation of air intakes for aerobic propulsion.

These two shapes are based on the hot-structure or uncooled concept considered before recent Langley studies of cooled structures were performed.

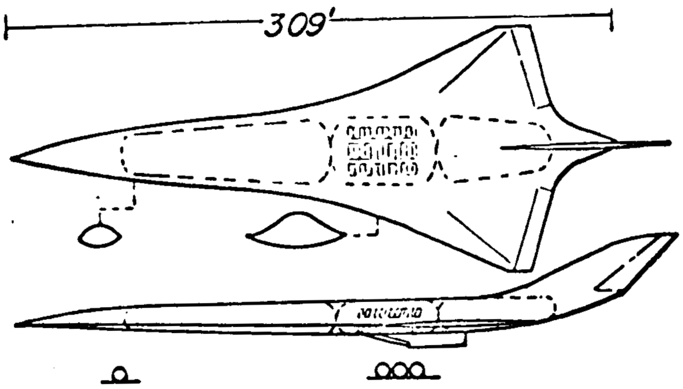

Figure 3. Configuration of the Langley HT 4 hypersonic transport

Whatever the project, prediction of the aerodynamic lift/drag ratio encounters difficulties not encountered in supersonic aircraft of the preceding generation. It is a matter of calculating non-viscous aerodynamic fields over three-dimensional shapes where linearized theory is not applicable.

Integrated shapes are more difficult to calculate in this respect than shapes with a round fuselage and a separate thin wing. Examination of these theoretical problems was done in [7].

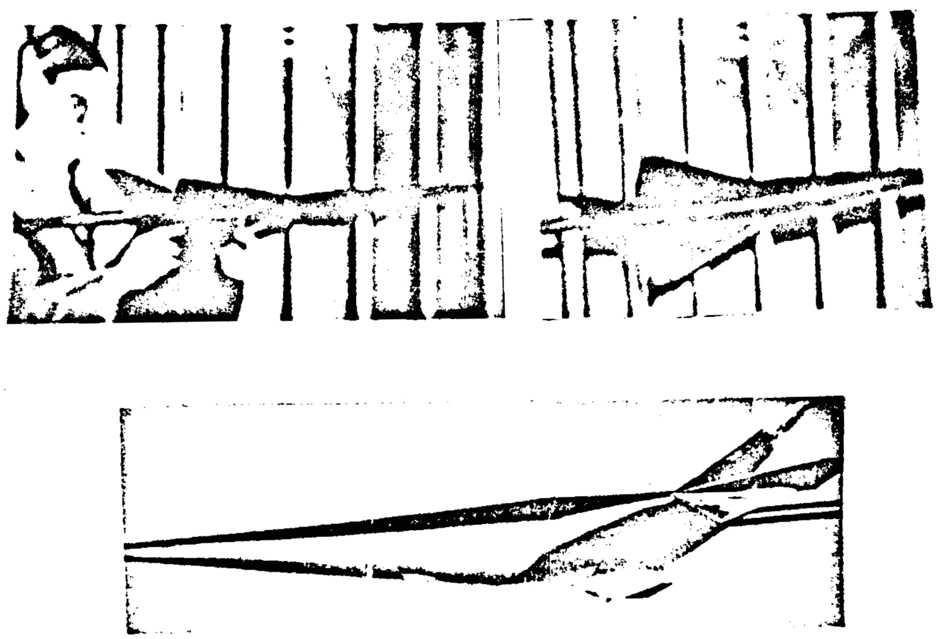

Figure 4. (Above) Wind tunnel test of Langley HT 4 model. (Below) Integrated configuration tested at Ames.

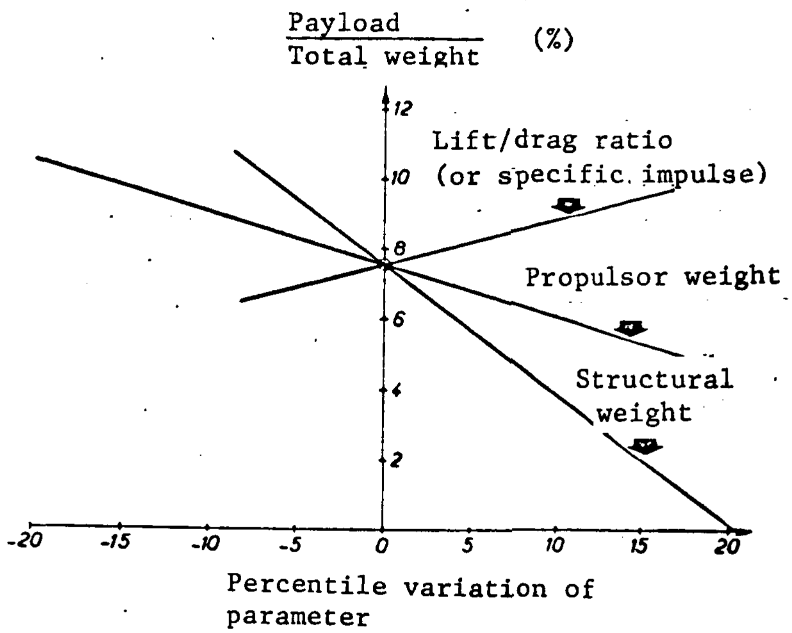

Figure 5. Hypersonic aircraft. Sensitivity of payload to various parameters.

Calculation of the three-dimensional boundary layer on an aircraft with incidence can be attempted for the bottom surface, by the prevalence method, for example. Even at very high /36 Mach numbers, turbulent flows are observed on the upper surface, accompanied by intense heating, which defeat simple calculations. Reference [8] is devoted to this study of turbulent flows on the upper surface of a 75° delta wing at Mach 2, 4, and 7. It contains many visulizations of flow at the wall, as well as strioscopic views of the general flow, with an important bibliography on leading-edge detachment on delta wings.

The second difficulty concerns applying wind-tunnel results to actual flight. Hypersonic wind tunnels currently reach Reynolds numbers such that the flow over the models is either laminar or transitional, while the Reynolds numbers corresponding to flight of 60 m aircraft are about 100 times greater. The respective figures are, for example, 2 to 3 million for a Mach 7 wind tunnel, and 200 to 300 million in flight. In addition, it is known that initiating the transition by roughness in a hypersonic wind tunnel is ineffective, and requires roughness dimensions such that the flow outside the boundary layer is strongly perturbed. Solutions to these difficulties have been investigated. As experimental study at Langley [5] used the Cornell shock tunnel with both high pressures and temperatures lowered to the point of liquefaction to obtain high Reynolds numbers. Figure 6 shows this for the HT 4 shape. It was then tested at Mach 8, but it is not certain that the turbulent pattern

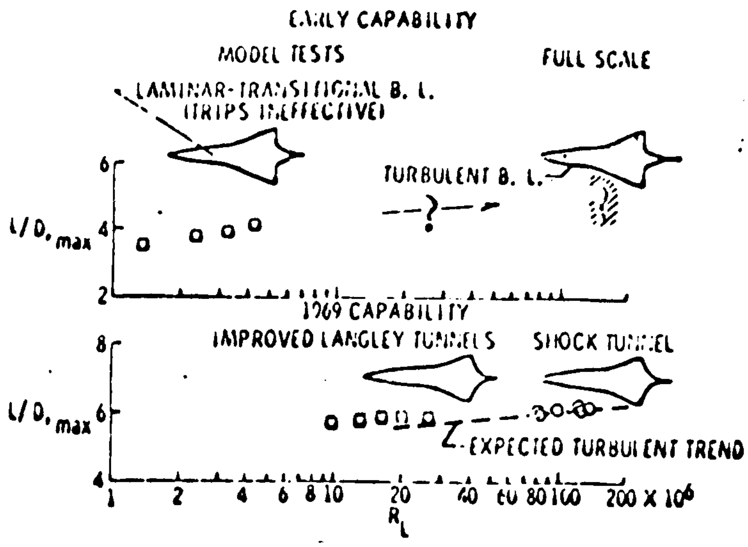

Figure 6. Recent progress in predicting the maximum lift/drag ratio in flight from wind-tunnel tests [5].

anticipated for the wind tunnel tests on smooth models will occur in flight on real aircraft with surface imperfections.

Although the creation of wind tunnels operating at very high Reynolds number is desirable, tests would encounter model deformation problems. Many aerodynamic studies useful to hypersonic aircraft projects are still possible in present aerodynamic wind tunnels, particularly studies of the configurations to be discussed below.

Lateral Stability

A hypersonic aircraft must necessarily traverse a large range of Mach numbers, so its configuration must be able to be balanced for takeoff at the maximum Mach number. The displacement of the center of thrust must thus be well-known, and as limited as possible. The plan shape plays a fundamental role in this regard. Figure 7 compares the aerodynamic center of three different shapes from subsonic to Mach 7. One of these is an ogee wing, the second a double delta, and the third a hypersonic L_1 configuration studied at ONERA.

The observed displacement of the center of thrust is very different for the different shapes: for the ogee wing it is continuous from subsonic to hypersonic, without rapid variation at transonic velocities. For the other shapes, the usual abrupt transonic decrease is observed. On the double delta,

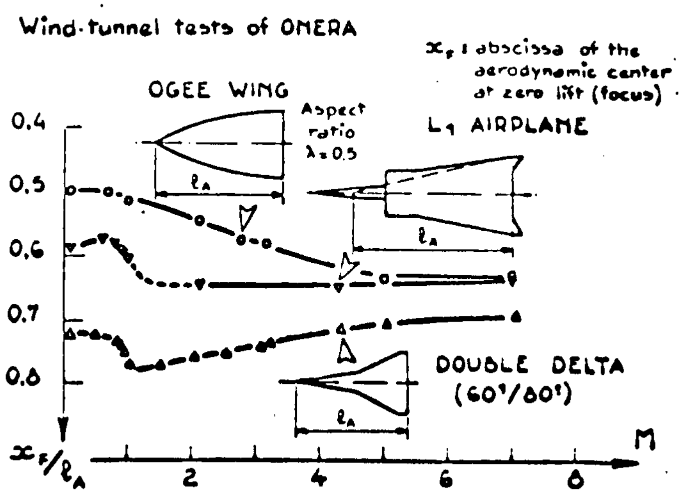

Figure 7. Effect of plan shape on focus displacement at high supersonic speed $0 < M \leq 7$.

the aerodynamic center then advances again toward its subsonic position, and this is in fact the advantage claimed for this shape.

The L_1 configuration, a photograph of which is shown in Figure 8, has no aerodynamic center displacement in supersonic flight.

It could thus be thought that a judicious choice of the plan shape — for example, the pure delta — would assure a minimum displacement of the center of thrust in supersonic flight, but in reality, depending on the curvatures of the wings considered, the center of thrust at flight incidence can be different from the aerodynamic center. Furthermore, at high Mach numbers, and on the thick wings which are sometimes considered, the phenomena cease being linear, and the effects of airframe camber (to fix the center of thrust) can no longer be treated separately from the symmetric effects of thickness. In fact, for increasing Mach number, it is the bottom /37
of the aircraft which progressively governs lift and moment. The variation in the ratio of $C_{z\ upper}$ to $C_{z\ total}$ for a thin plate at 10° incidence with increasing Mach number shows this clearly (Figure 9).

The displacement of the center of thrust for variable Mach number is already a major preoccupation in present civil supersonic aircraft projects, for which it is necessary to provide, for example, complex pumping systems to displace fuel or water forward to aft to maintain the center of gravity permanently at a proper distance from the center of thrust. In a hypersonic aircraft, the problem will be complicated by the more severe thermal environment.

Influence of Engines on the General Aerodynamic Properties

In the case of present supersonic transport aircraft, considerations of heating and structural life have dictated the choice of metal, its grade, and even the machining methods used. These difficult problems can be resolved without great repercussions for the aerodynamic design. Likewise, the propulsor is developed independently, and the aerodynamic solution can be handled fairly freely.

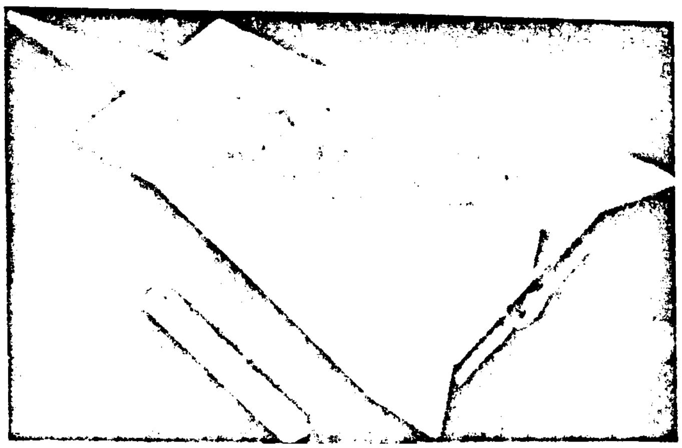

Top view

In the case of a hypersonic aircraft, each area of its development is intimately connected to the others. The type of structure and its type of cooling will be different for hydrogen scramjets, which require a large and fragile fuselage (liquid hydrogen

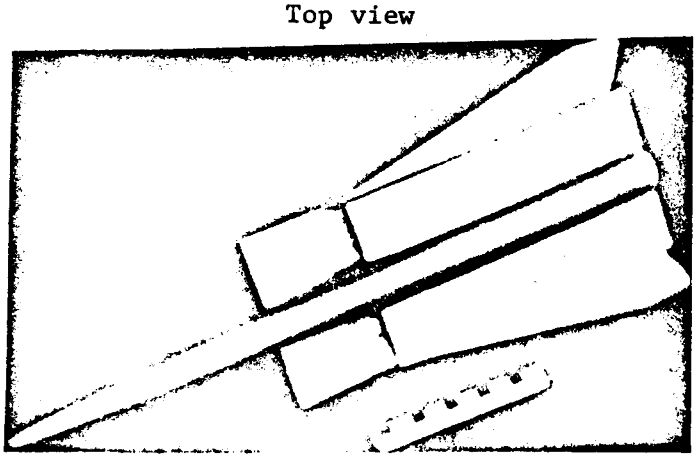

Bottom view

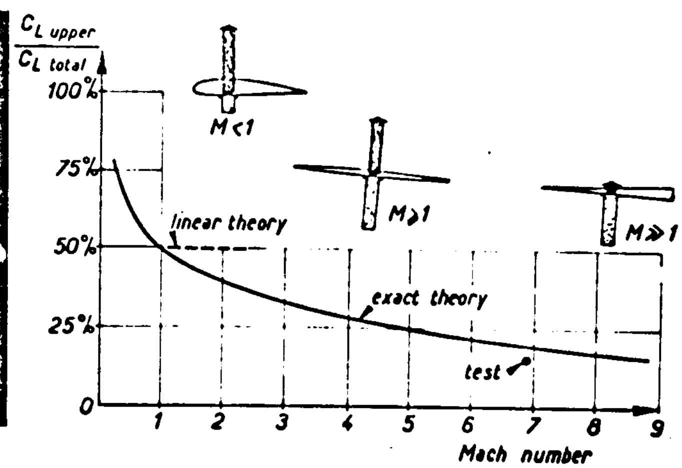

Figure 8. Aerobic hypersonic aircraft. Two-dimensional air intake and exhausts. 1/175 model for wind tunnel test of the configurations.

Figure 9. Contribution of upper surface to lift of wings at high supersonic velocities. (10° incidence)

has 2.5 times more energy than kerosene and about 10 times lighter), and for turborams — a rocket mounted in a large fairing coupled to a fuselage of more modest dimensions containing kerosene and liquid oxygen.

Under present conditions, it seems difficult to undertake a general optimization study in a valid manner.

Without claiming optimization, one can attack the aerodynamic problems by choosing one or more projects which preferably represent extreme configurations, and submitting them to an investigation which includes calculations and wind tunnel tests. One can thus hope to show the validity limits of existing methods of calculation, discover unsuspected problems, and collect experimental lift data which are general enough to assist in the design of new projects.

This route is, of course, being followed by NASA in its two principal centers, Langley and Ames. Figure 4 shows, above, the HT 4 model tested at Langley, and below, the integrated-wing model tested at Ames. On the first model, the engine nacelle seems to have moderate dimensions; this impression is due to the relative large size of the fuselage containing liquid hydrogen.
In all the designs, the engines are located under the wing to benefit from /38
the compression by the under surface. Another evident advantage of this arrangement is the almost complete attenuation of local incidences ahead of the air intake during variations in the incidence of the aircraft. These apparent benefits must, however, be compared to disadvantages due:

a) to the presence of the boundary layer of the wing;
b) to a flow field which is not perfectly uniform;
c) to the effects of a curved shock wave on the internal flow.

The study of these three effects interests air intake specialists, and will not be discussed here.

Figure 10 shows the relative dimensions of the air intake and exhaust

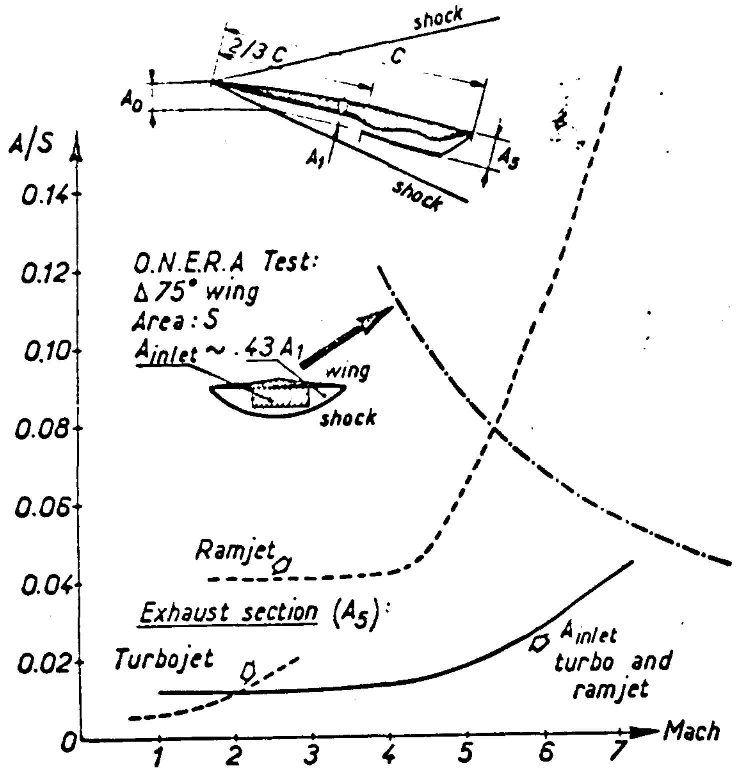

Figure 10. Aerobic aircraft. Increase in intake and exhaust sections of turbojet and ramjet engines at high Mach number.

sections necessary for a turbojet or a ramjet using kerosene, expressed in the percentage of the surface of the wing under which the engine is placed.

The figure also compares the available section, taken equal to 43% of the section between the wing and the shock; this is for a 75° delta wing flying at C_z = 0.1. The plane of the air intakes is located at 2/3 of the central chord; the wing loading is 300 kg/m^2 (61 PSF). The hypotheses concerning the aerodynamic lift/drag ratio of the aircraft and the unit thrusts of the engines out to Mach 3 are those of a present SST. The estimated unit thrusts of a ramjet and the lift/drag ratios anticipated beyond Mach 3 are given in Table I.

TABLE I

M	3	4	5	6	7	8
C_z/C_x	6,8	6	5,5	5	4,5	4
T/A •	4000	3500	2700	2300	1700	1150

• T/A Frontal-area thrust in kg/m^2

In Figure 10 one may see a considerable increase in the intake surface for M > 4, to the point that, toward M = 7.5, the intake occupies practically all the available section, assumed equal to 43% of the section between wing and shock.

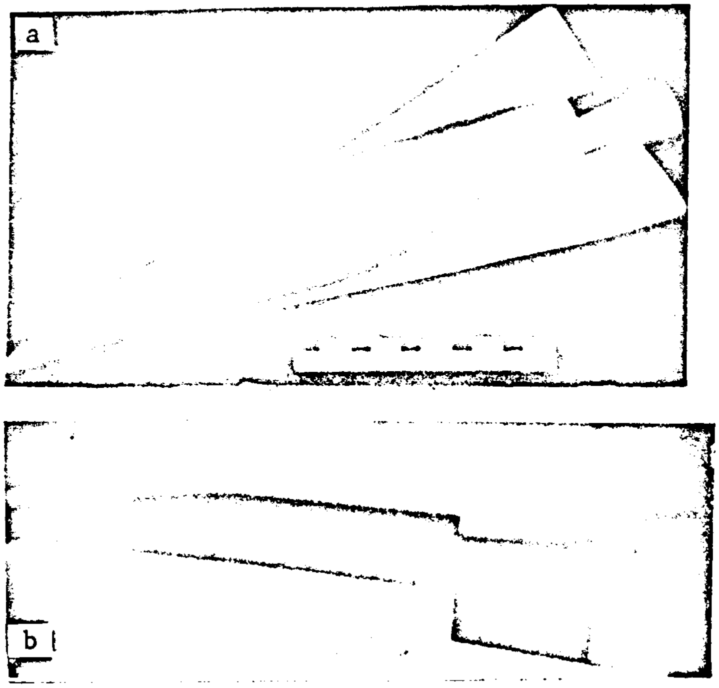

Figure 11. Experimental hypersonic vehicle tested at ONERA.

a) Photograph of model;

b) Strioscopic view: Mach 7, 5° incidence.

Figure 11 shows a photograph of an experimental hypersonic vehicle studied in an ONERA wind tunnel. The strioscopic view, made at Mach 7, at 5° incidence (corresponding to the maximum lift/drag ratio) shows that the shock wave of the wing is already near the supersonic ramjet air intake despite its very far-back position. Tests for this project have shown that the ramjet is sufficient to assure course stability.

It thus seemed interesting to conduct wind tunnel tests on several configurations of hypersonic aircraft with air-breathing engines of various types to show the contribution of large engines to the general aerodynamic properties. Figure 8 shows a model of such an aircraft equipped with four turboramjets arranged in pairs in two large nacelles. The nacelles of the model are "transparent" — that is, they contain a channel of constant section between the intake and the exhaust, in order to assure that during wind tunnel measurements there is a supercritical configuration simulating the normal operation of the air intakes. /39

The fuselage is very slender, and the leading edge of the wings is swept at 79° to reduce heating and drag. A rectangular precompression ramp is located ahead of the air intakes. This model has been tested from M = 0.6 to M = 7 by ONERA [9] (a second, larger model has been tested at takeoff and

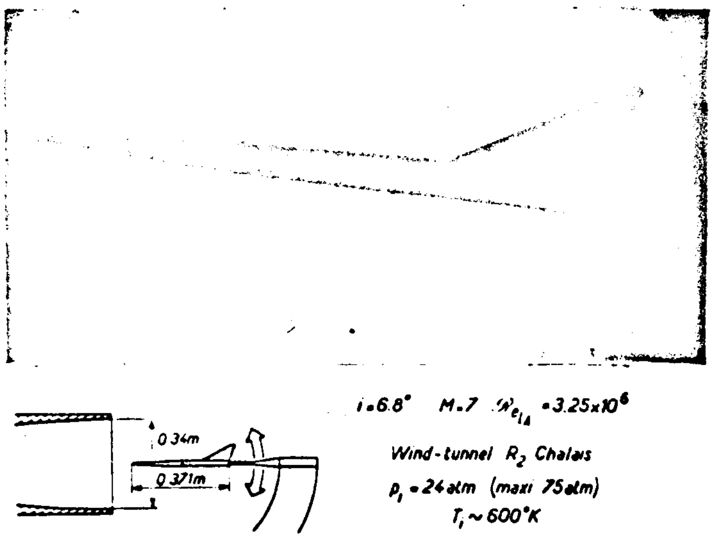

Figure 12. L_1 hypersonic aircraft. Strioscopic view at Mach 7.

landing velocities in a subsonic wind tunnel). Figure 12 gives a strioscopic view of the flow at Mach 7 in the ONERA wind tunnel R2 at Chalais. It is significant that the only shock waves visible are those issuing from the edges of the air intakes. Calculations have shown that their contribution to the total drag is really very large, and that the leading-edge radii of the intakes must be reduced to a minimum if one wishes to obtain an acceptable aerodynamic lift/drag ratio for the aircraft. It is possible to attain this by means of active cooling, as has been proved experimentally (see [10] and [11]).

Influence of Engines on Transverse Stability

The model has undergone tests of course stability with and without engine nacelles, at different incidence angles and at different Mach numbers, to isolate the contribution from the engines. Figure 13 shows that at Mach 2.12, as well as at lower Mach numbers, the presence of nacelles increases the course stability as a function of incidence. At M = 4.29, the effect of the nacelles is small and scarcely dependent on incidence. At M = 7, increase in incidence increases the unfavorable effect of the engines. For each Mach number the center of measurement was fixed so that the aircraft would be slightly stable longitudinally.

Another concept of the same project has been tried.

Figure 14 shows that the large nacelles of turboramjets have been replaced

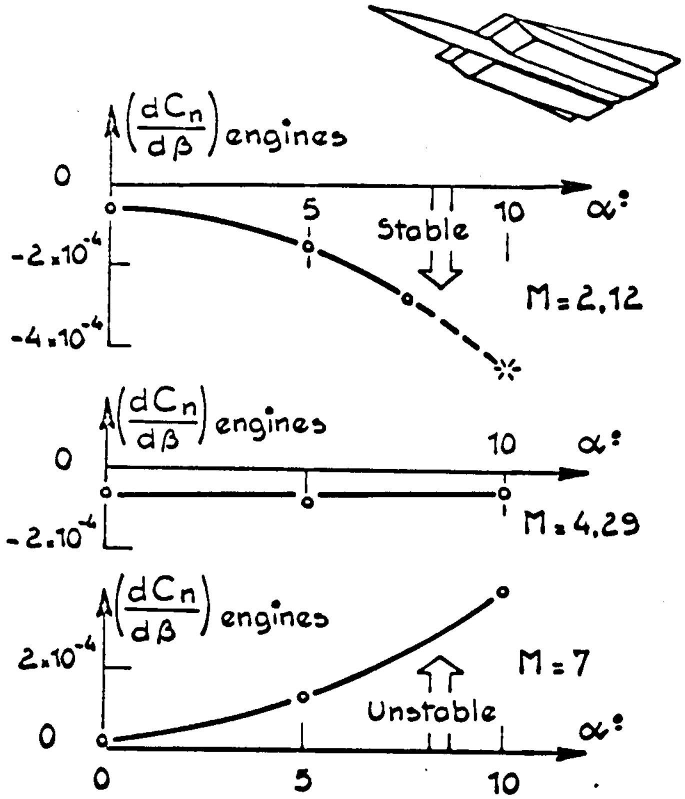

Figure 13. Influence of engine fairings on course stability of a hypersonic aircraft. ONERA tests.

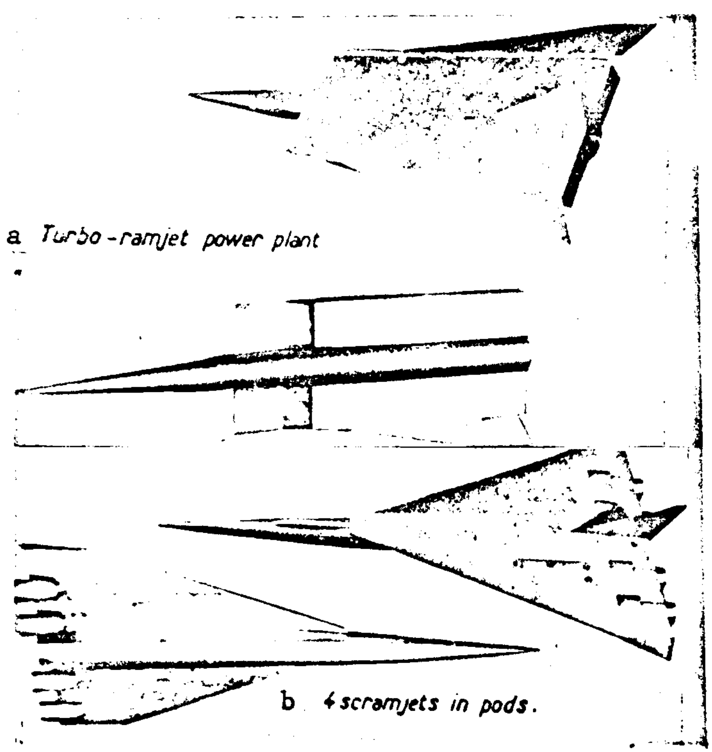

Figure 14. Hypersonic aircraft: influence of engine option on configuration.

a - turbo-rams coupled to fuselage;
b - ramjets with supersonic combustion (Scramjets) hung under the wing.

by four supersonic ramjets. The wing is a 68° delta to offer a sufficient air-intake section between the lower surface and the shock wave out to 10° incidence. The wing tips are bent downward to increase the course stability with incidence, while the fin surface has been reduced by half.

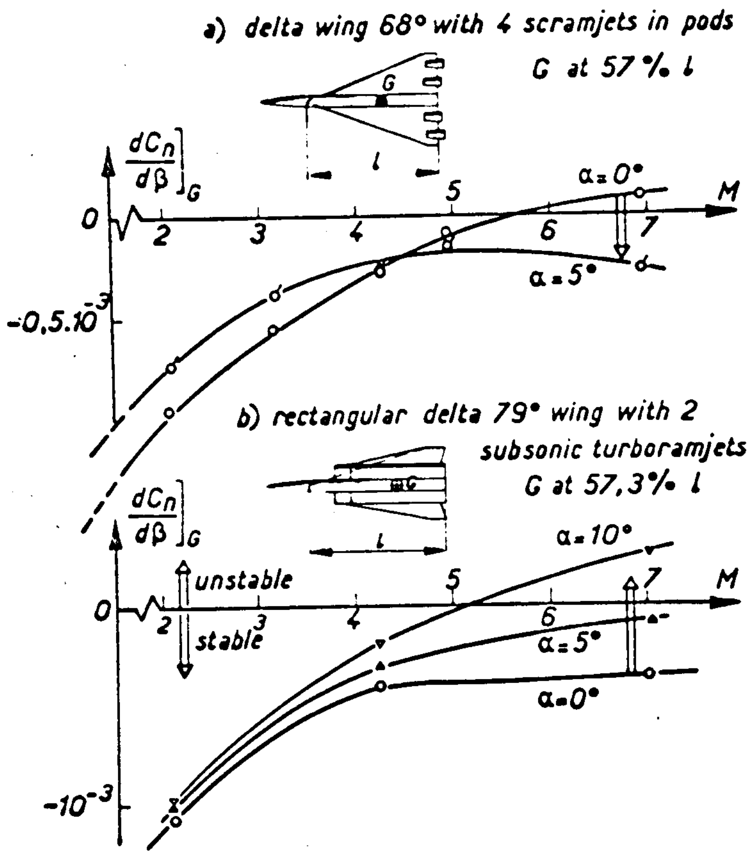

Figure 15. Influence of engine type on course stability. ONERA tests.

Figure 15 compares course-stability curves, in which the requirement of an acceptable longitudinal static margin is retained for the two configurations.

Comparison of the results shows that the scramjet configuration loses its stability at zero incidence for M of about 6, but remains stable at flight incidence near 5°. At this incidence the presence of scramjets seems unfavorable for M about 4, and favorable beyond that. The turboram aircraft, on the other hand, is stable at zero incidence, but with nonzero incidence the effect of the engine nacelles is always unfavorable, and beyond Mach 5 a maneuver with a large loading factor would be catastrophic.

Figure 16 compares the Mach 7 course stability of the two configurations with and without their engines. The influence of the scramjets mounted under

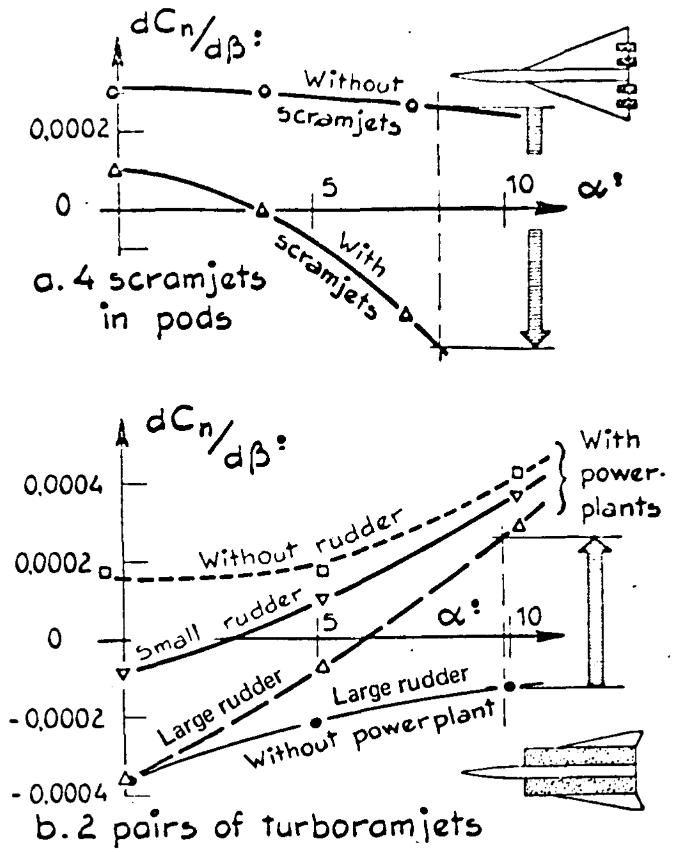

Figure 16. Influence of engine fairings on the change in course stability with incidence at M = 7.

a) 4 suspended Scramjets

b) 2 pairs of coupled turborams.

the rear of the wing is clearly confirmed as the source of the stability in incidence. In contrast, the turborams reduce the stability. The tests have been repeated on this latter /40 configuration without a fin and with fins of different surface shapes. Without engines, the stability of the aircraft equipped with the large fin decreases progressively, but remains stable up to the maximum incidences tested. This influence of the engines on the course stability is similar to the results of slender-body theory. In this theory the lift of a hollow cylinder is localized on its forward face. Thus, if the air intake of the engines (supercritical) is located far ahead of the center of gravity of the aircraft, the resultant lateral force from going into slip will produce an unfavorable course-stability gradient. Inversely, the air intakes of the scramjets, moved back behind the center of gravity, will produce a favorable gradient of the yaw moment. Likewise, the influence of the incidence can be reduced to that of the local kinetic pressure under the wing: q_1. Assuming implicitly that the ratio of specific heats does not vary, pressure q_1 increases with incidence in the ratio(2)

(2) It is implied that the ratio of specific heats is constant: $\gamma_1 = \gamma_0$

$$q_1/q_0 = (p_1/p_0)(M_1/M_0)^2$$

where p and M are the static pressure and the Mach number, and the indices 0 and 1 refer to upstream and local conditions, respectively.

These remarks suggest that to reduce the drag, one should choose the position of the engine nacelles so that they contribute as well as possible to the course stability, when the fin surface can be reduced to the minimum /41
imposed by requirements for stability in subsonic flight.

Conversely, one can hope to reduce the influence of the air intakes on the course stability by placing them in the immediate vicinity of the center of gravity. For the relatively short engines considered for aircraft using liquid hydrogen, this then poses the problem of the influence of the jet from the nozzles on the after part of the aircraft.

Problems of the Interaction of the Propulsive Nozzles

For present-day supersonic aircraft, adapting ejector nozzles to the different altitudes and velocities of the mission already requires considerable variations in the shape and section of the jet. These variations naturally aim at obtaining the best propulsion efficiency. Since the cross section is maximum at the maximum Mach number of flight, the jet must be confined at transonic and subsonic velocities. If the boattail does not follow judicious laws, and especially if it violates the area law too grossly, it can produce transonic problems.

For a hypersonic aircraft, the problem raised by this necessary variation of the after shapes becomes more acute for two reasons:

(a) To fly from subsonic to a high Mach number, for example M = 7, requires variations in section which can no longer be obtained by present axisymmetric systems (so-called "iris"), but rather by two-dimensional nozzles with a single variable baffle;

(b) The local aerodynamic field is more complicated. Figure 17 is a schematic representation of the after portions of a present-day fighter and of a hypothetical hypersonic aircraft. The pressure around the rear section of the Mach 2 fighter is not significantly different from the pressure at infinity upstream, and adaptation can remain axisymmetric. For the high-Mach aircraft, at Mach 7 and flight incidence of 5°, local pressures on the under and upper surfaces of the wing — thus, at right angles to a two-dimensional nozzle located at the aft end of the aircraft — can differ by a factor of 5 ($P_{under}/p \approx 2.3$; $P_{upper}/p \approx 0.4$).

Change in Mach number or maneuvers with high load factor must thus be accompanied by asymmetric deformations of the ejection nozzle. Now, the aerodynamic forces which act on the air intakes and exhausts are very large; in particular, the forces applied to the ejector nozzle at large Mach numbers can be on the order of the aircraft weight. The moments of these forces can thus become a very important element in the longitudinal stability of the aircraft. Variations in these moments related to changes in engine operating conditions, to asymmetric detachments during maneuvers, or to accidental flameout, must be capable of being controlled by the control surfaces of the aircraft.

Figure 18 shows the result of calculations on the thrust vector of different two-dimensional nozzles, and shows the influence of the opening angle /42
on the direction of this vector. It can be seen that the uniform-field nozzle leads to an inclined thrust vector. It can be seen that the uniform-field nozzle leads to an inclined thrust vector (because of the suppression of part of the lower plane), and that its line of action lies about 30 throat-heights above the lower plane. These calculations are for a perfect gas with $\nu = 1.4$, where F_∞ denotes ideal thrust in a vacuum.

The best integration of engine to airframe will thus have to depend, in each particular case, on wind tunnel tests with representation of propulsive

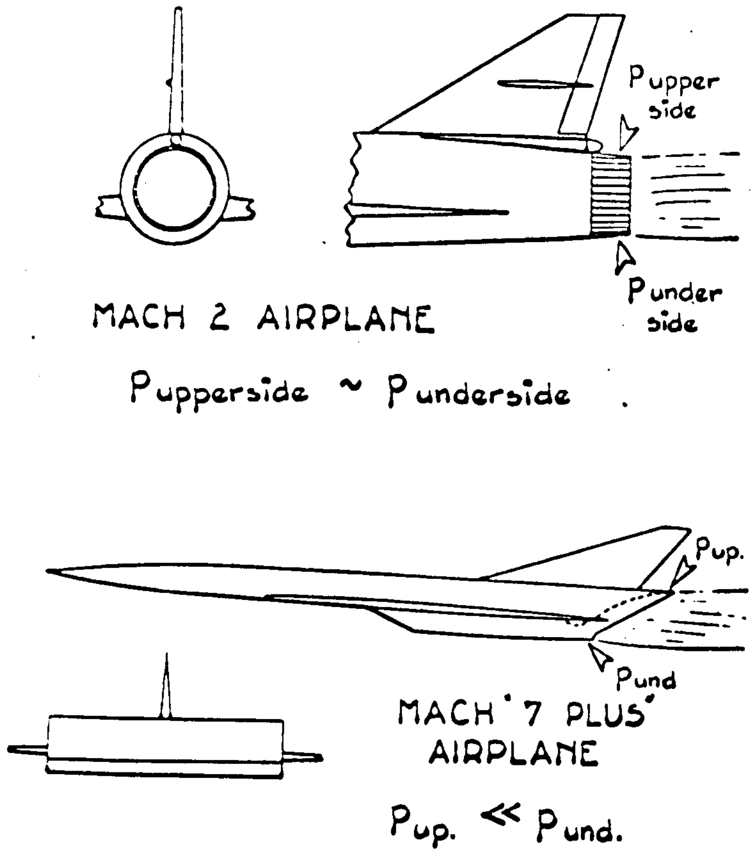

Figure 17. Adaptation of propulsive nozzles to external aerodynamic field.

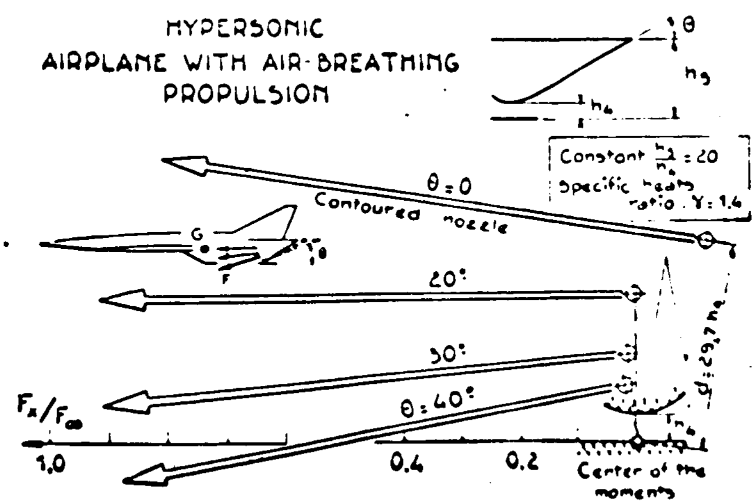

Figure 18. Influence of angle of two-dimensional nozzle on direction of thrust.

jets [12] contains an example of such tests performed at Langley, which show the effect of the jet on the moments of an aircraft.

Even more than in modern supersonic aircraft projects, the large relative dimensions of future hypersonic aircraft engines will require that the internal circulations be represented with great fidelity during wind tunnel tests, since the effects and interactions of the propulsive fluid will play a large role in the forces and moments acting on the aircraft.

Aerodynamic Elasticity Effects

Recent years have seen the appearance of a certain number of problems related to large differences between aerodynamic properties deduced from wind tunnel tests of rigid models and those observed in the flight of real elastic vehicles.

One can mention the differences found in the yaw moment induced by aileron settings ($dC_n/d\delta_A$) on the Mach 3 XB 70 A bomber [13], where the sign of the moment observed in flight at M = 0.95 (Figure 19) was opposite to that measured in the wind tunnel, and even the case of the Apollo capsules where the equilibrium angle observed in flight differed from that measured in the wind tunnel because of deformation of the heat shield under loading (Figure 20, from [14]).

After considering the effects of Mach number and Reynolds number, correct models of the Apollo capsule were made, where the elastic deformation of the heat shield was represented, and the new values of the equilibrium angle fell exactly among the flight points.

For aircraft of large dimensions with very light structures, and in the presence of a severe thermal environment, it can be predicted that this problem will be even more important, and that to be significant, wind tunnel tests will have to use models reproducing as well as possible the deformations expected in flight.

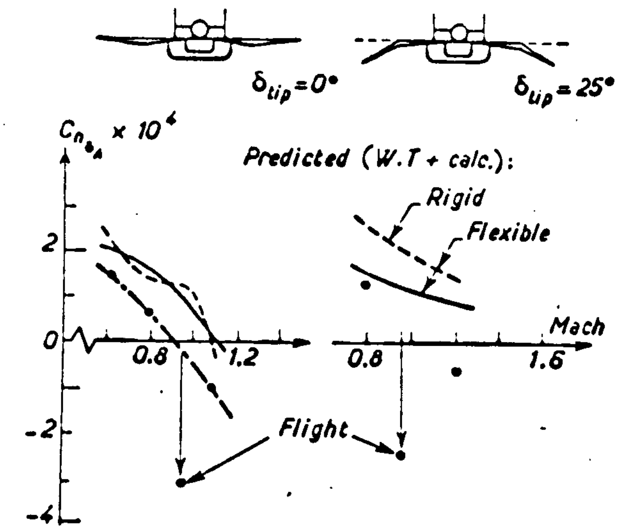

Figure 19. XB-70 A — Influence of structural elasticity on oscillation induced by ailerons.

Aside from the aerodynamic questions raised by the configurations of hypersonic aircraft, a certain number of elementary problems remain, which require solution before proceeding to configurational design.

The most important of these, perhaps, is that of control surfaces.

The problems of the effectiveness and heating of aerodynamic control surfaces of re-entry gliders at hypersonic velocities and at high incidences have been studied for many years, and recognized to be very difficult. This comes in part from the theoretical complexity of the viscous and nonviscous flow fields considered, and partly from insufficient simulation in present-day hypersonic wind tunnels.

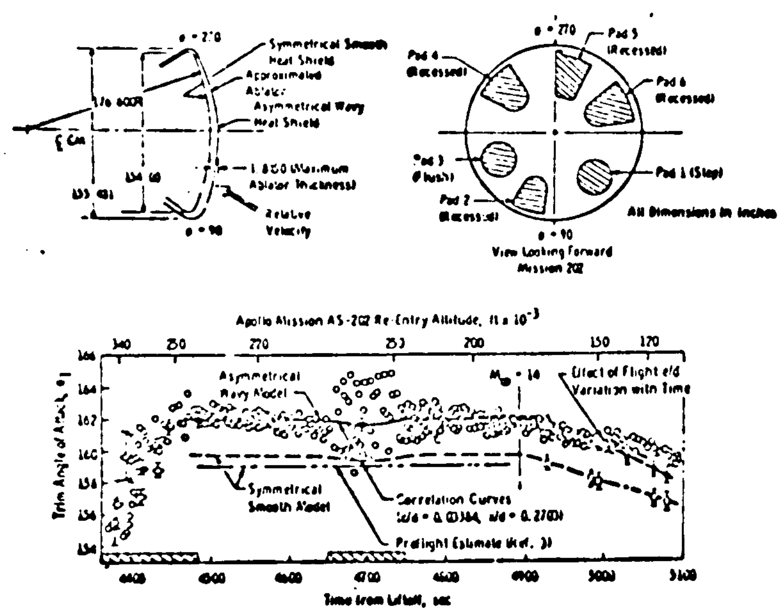

Figure 20. Deformation of Apollo heat shield: influence on equilibrium incidence.

But these difficulties exist even in the apparently simpler case of a hypersonic aircraft with relatively sharp leading edges and thin wings, flying at low incidence, conditions obligatory for obtaining high lift/drag ratio. An aircraft 60 m in length with normal wing loading will be surrounded by a turbulent boundary layer over almost all its surface. In addition, classical considerations based on simple oblique shock theory are insufficient to estimate the compressions and expansions on control surfaces attacked by thick boundary layers. It can be expected that the local boundary layers will govern the course of the expansion and compression, and thus the effectiveness and the heating of the control surfaces.

Unfortunately, wind tunnel testing of small-scale models inevitably shows laminar detachments. Figure 21 shows a number of results concerning flow detachment on bent flaps. One can see two well-separated groupings when one plots the factor $\alpha_i M^{-1/2}$ as a function of the Reynolds number at the hinge, where α_i is the setting where detachment occurs, and M is the local Mach number outside the boundary layer. It can be determined that in the conditions of turbulent flow corresponding to flight, large settings, on the order of 30°, are possible without detachment, while for a wind tunnel test, in the presence of a laminar boundary layer — for example, for Re = 2×10^6 and M = 8 — the allowable setting is limited to 5° or 6°.

These circumstances explain why most of the research on heating and effectiveness of control surfaces at hypersonic velocities has rapidly deviated toward the study of laminar detachment ahead of dihedra, while the study of control surfaces under realistic conditions has advanced little. To try to make progress on this question, ONERA has undertaken a study of the compression of hypersonic turbulent boundary layers on a control surface [15].

The theoretical study has consisted of applying the characteristic method to the boundary layer approaching the flap; for this, the boundary layer is considered to be a nonviscous rotational layer.

The idea of assuming that the abrupt change of a turbulent boundary layer could be compared to a nonviscous phenomenon, since pressure effects are

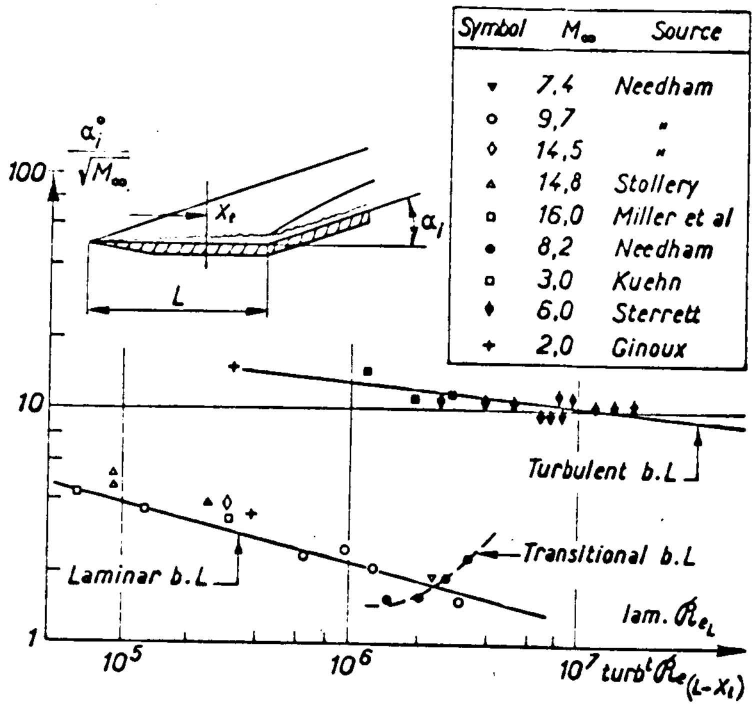

Figure 21. Maximum flap setting (α_1) before appearance of detachment.

preponderant there, has been expressed by P. Carriere and M. Sirieix [16] and applied by various authors to treat shock reflections [17] or compressions on a ramp [18].

An experimental study was conducted in the R3 wind tunnel at Chalais-Meudon at Mach 10 to verify this point of view. It used a long flat plate (Figure 22) placed in the symmetry plane of the tunnel; small plates representing the bent flaps were /44 attached to the back edge of this plate, where thick turbulent boundary layers corresponding to Reynolds numbers of 13 to 20 million were produced. The theoretical and experimental details are given in [15]. Figure 23 illustrates the test conditions. The strioscopic view at the upper right is taken from a previous study [19] made in 1966 in the same wind tunnel (R3) on a short plate. The study was marked by the inevitable laminar detachments; the enlarged photograph below it shows the laminar boundary layer which can be followed out to its re-attachment to the flap.

The two lower strioscopic views show, in contrast, a very pure configuration where one can distinguish clearly, at the very interior of the thick turbulent boundary layer, the origin of the shock included in the calculation of the characteristics. The outer edge of the boundary layer, quite visible in the original photographs, has been enlarged here for clarity of reproduction; this edge meets the oblique shock farther from the flap hinge as the setting

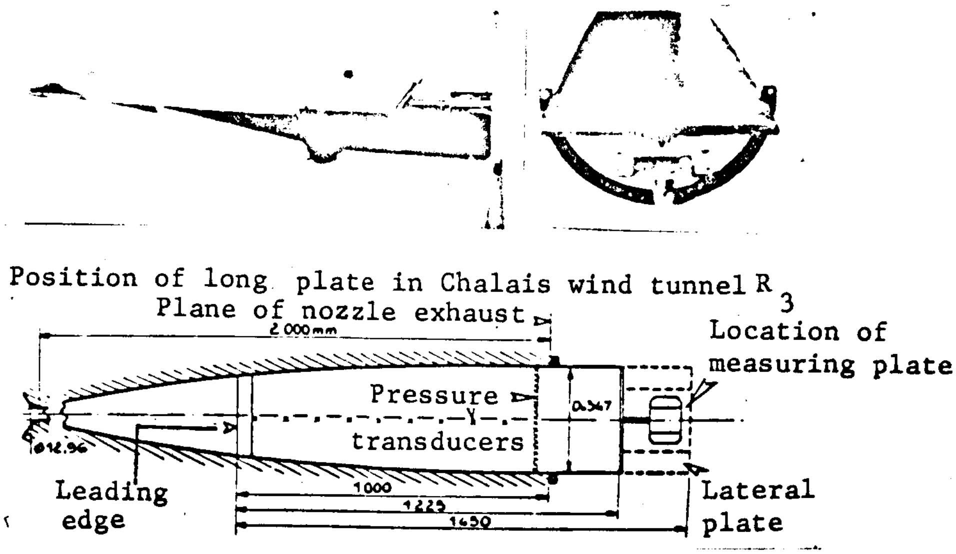

Figure 22. Long median plate.

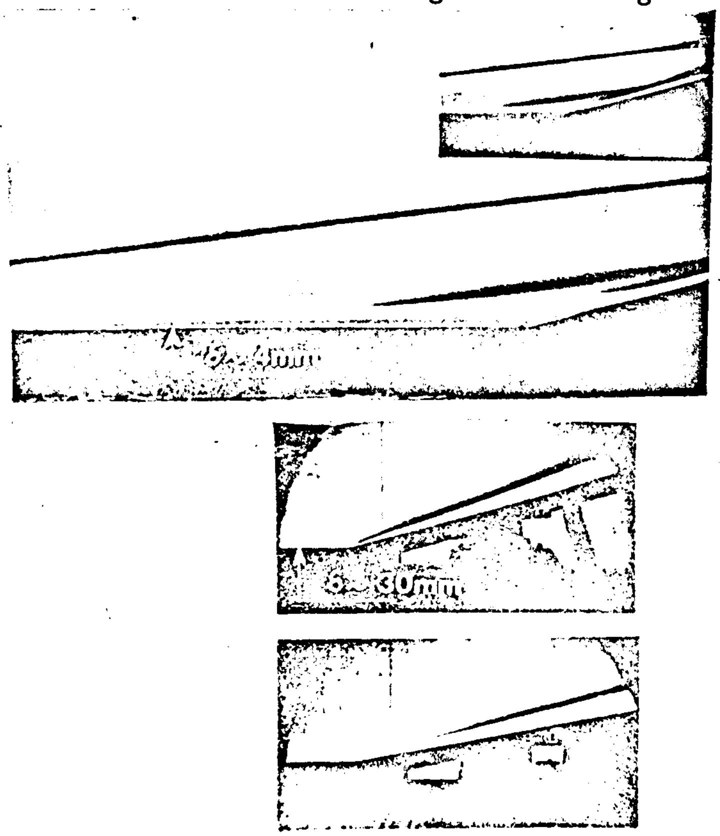

Figure 23. Compression on a bent flap at Mach 10 (Chalais wind tunnel R 3)
above: detached laminar boundary layer;
below: nondetached turbulent boundary layer.

decreases. This explains the very spread-out recompressions recorded by the measurements of pressure distributions.

Figure 24 compares the results of calculations made this way by the method of characteristics with those from two-dimensional oblique shock theory, and with the first measurements of pressure made during this program. It may be seen that the compression on the flap is more spread out at smaller angles. It is in this region of small settings that the difference between the real effectiveness of the flap and that obtained by oblique shock calculations is most marked. In contrast, at higher settings the compression is more rapid: for $\alpha = 25°$, for example, it is established on a length of 60 mm, or about two thicknesses of the boundary layer at the hinge ($\delta_0 \approx 30$ mm) with the present experimental conditions.

The calculation for $\alpha = 30°$ was interrupted by the appearance of a local Mach number less than 1 at the lower edge of the flow, which stops the present computer program.

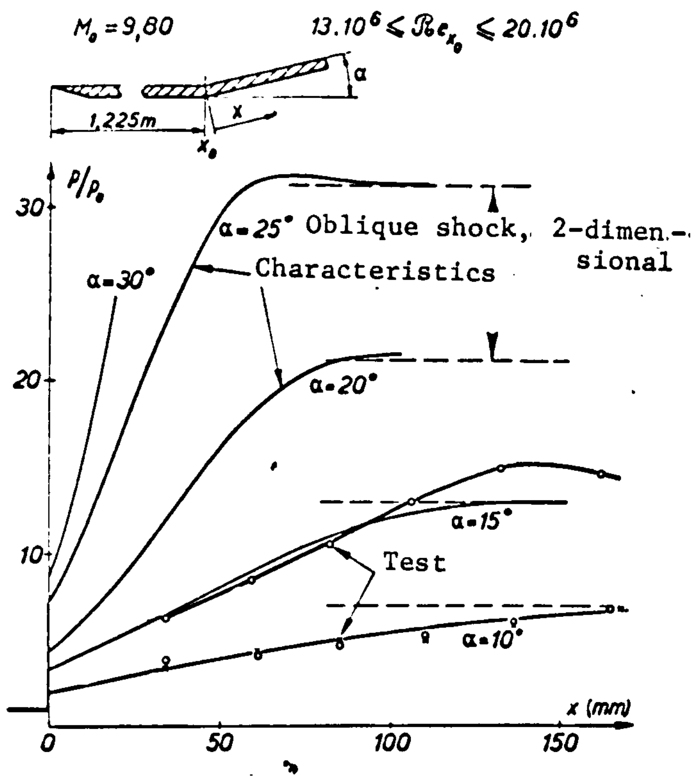

Figure 24. Recompression on a bent flap. Turbulent boundary layer: $\delta_0 = 27$ mm

Figure 25 compares two measurements and two calculations made for experimental conditions (plate length and generating pressures) leading to different boundary-layer thicknesses. It can be seen that the lengths of compression on the flap are different. Plotted as a function of the reduced abscissa X/δ_0, the two experimental results fall quite well on a single curve, showing that the boundary layer does indeed fix the scale of the recompression, just as the theoretical outline implied.

One experiment, designed to obtain measurements of the effectiveness of flaps on a model of a hypersonic aircraft tested at Mach 7 by ONERA, has been carried out in the R2 wind tunnel at Chalais-Meudon.

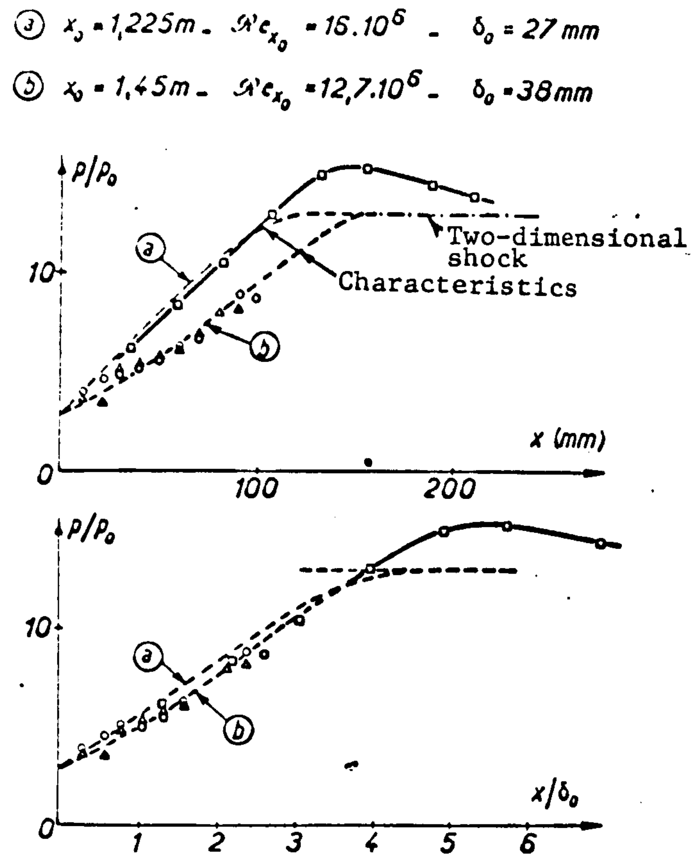

Figure 25. Pressures on a flap set at $\alpha = 15°$. Chalais wind tunnel R 3, M = 9.80

Figure 26 shows the design of a model where the flaps are equipped with pressure transducers. /45
Calculations by the characteristics method have as a departure point the boundary layer calculated as if it were turbulent starting at the sharp leading edge(3).

There is good agreement between measurement and calculation. Here again the real effectiveness is much less than that predicted by simple oblique shock calculations.

Heating

Measurements of heating, carried out in parallel with pressure measurements at Mach 10 on thin-walled platelets (e = 0.5 mm) equipped with thermocouples 0.1 mm in diameter, are reproduced in Figure 27; the heat flow has a wavy behavior, in contrast to the monotonic behavior of the pressures.

Tests at a higher setting ($\alpha = 20°$) given in Figure 28 show that the heating produced a sinusoidal deformation of the thin wall, the effects of which are visible in this strioscopic view.

---

(3) The strioscopic views not reproduced here show, by the absence of detachment at the flap hinge, that this was effectively the case.

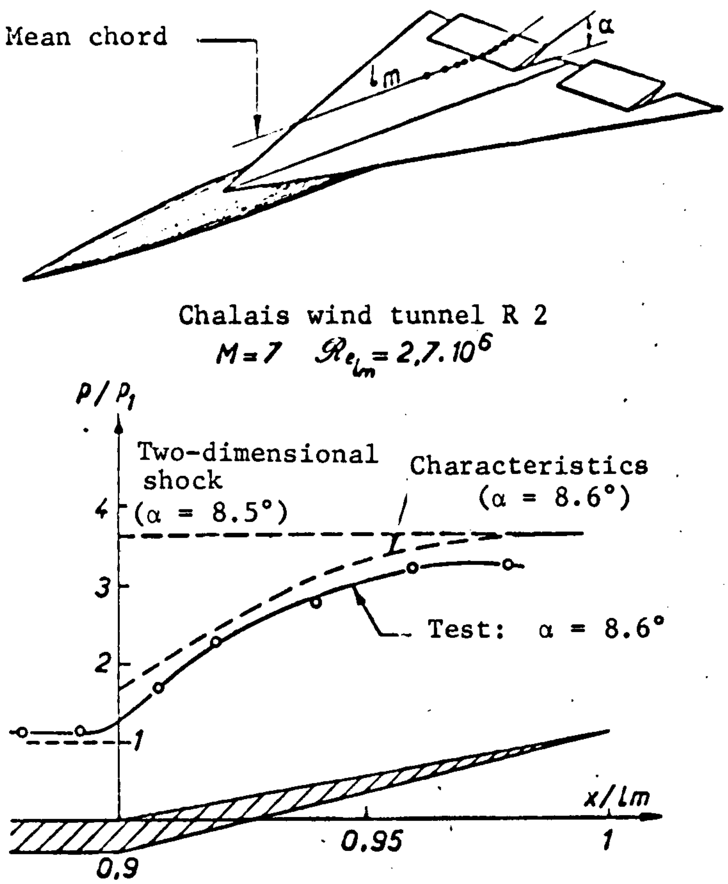

Figure 26. L 3 hypersonic aircraft — swept at 70° (zero incidence)

This deformation measured in the laboratory is shown in Figure 29. Calculations of local pressures have thus been obtained by taking this wavy shape into considera- tion (the flap is repre- /46 sented here in its true size). One can see the great influence of this small waviness on the cal- culated pressures, whose behavior closely follows that of the flux. The study was continued up until this report was written. It will include an attempt to calculate the viscous boundary layer from the calculated pressures, or at least to evaluate the fluxes. But it can already be assumed, on the basis of the present results, that the surface irregularities of a hypersonic vehicle, even though they are small with respect to the boundary-layer thickness, could produce considerable perturbations in the heat transfer, which could thus depart from the values of "smooth flat plate" theory.

Knowledge of the Hypersonic Boundary Layer

The exact physical properties of turbulent hypersonic boundary layers are far from being completely understood, even for the most simple cases of plane two-dimensional plates, as is shown by the number of papers published on this subject.

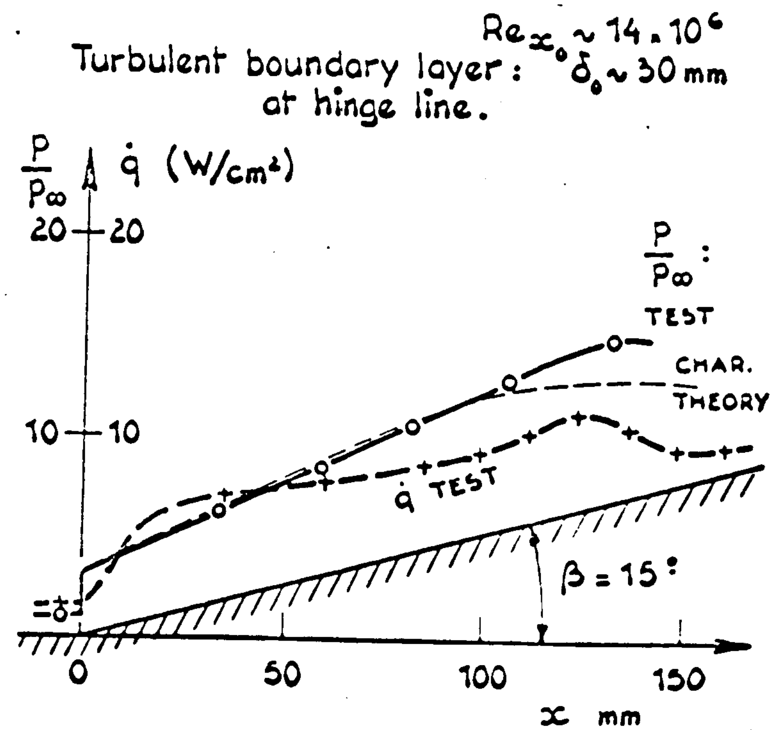

Figure 27. Distribution of pressure and heat flux on a flap set at 15° at Mach 9.8. ONERA wind tunnel R 3 at Chalais.

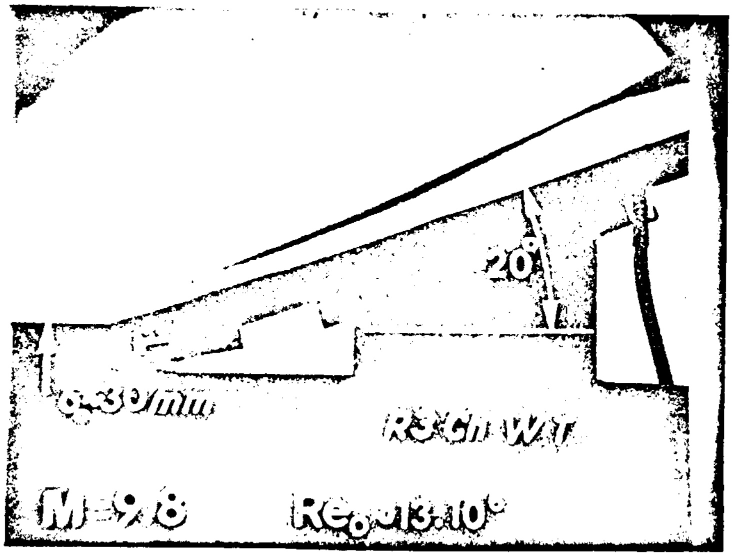

Figure 28. Strioscopic view of flow at M = 9.8 on a flap set at 20°, with deformed wall.

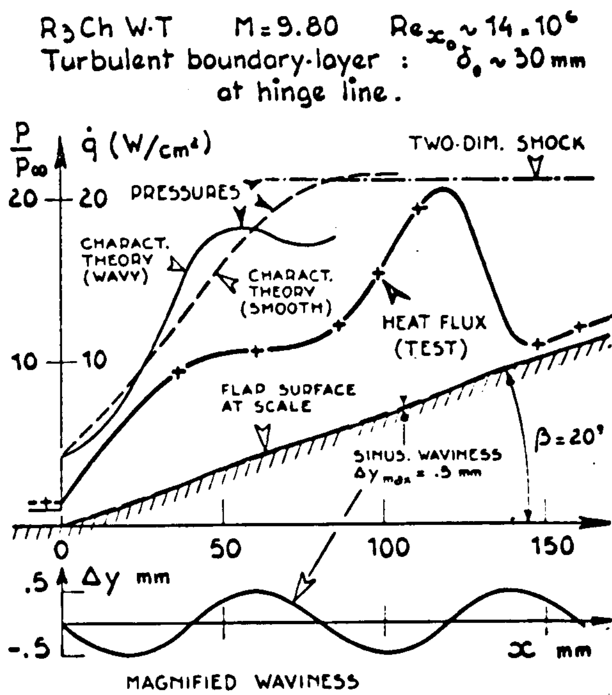

Figure 29. Pressures and heat fluxes at M = 9.8 on a flap set at 20°; influence of surface deformation.

Prediction of the development of the boundary layer on three-dimensional shapes with incidence will be even more complicated. Knowledge, even approximate, of the local boundary layers on the vehicle will be needed, not only to evaluate the effectiveness of control surfaces, as we have seen, but even to evaluate the thermal flux map on the whole aircraft.

In this respect, the problem of transition to hypersonic velocities will play a large part in the prediction of thermal constraints in a nonablative metallic structure. Knowledge of the exact numerical values of local Stanton numbers will be necessary to define the insulation of the cryogenic reservoirs and to conserve the maximal structural efficiency.

The present state of hypersonic boundary layer studies in Europe has been reviewed recently by R. Michel [20]. These studies are very promising and could contribute very effectively to the development of hypersonic aircraft.

Conclusion

Construction of hypersonic aircraft poses formidable problems in propulsion and in structure; however, they must not hide the aerodynamic problems which can only erroneously be considered secondary or trivial.

To aerodynamic studies of configurations, executed in classic fashion for the whole project, the following new studies will be added:

— obtaining measurements at high Reynolds numbers to try to obtain realistic turbulent boundary layers, and to learn the real lift/drag ratios which control the economics of the aircraft;

— conception and development of special mountings for wind tunnel tests incorporating a correct representation of the propulsive jets, on models representing the exact shapes of vehicles deformed in flight;

— improved knowledge of kinetic heating;

— dynamic and thermal studies of control surfaces in the presence of thick turbulent boundary layers.

These long and difficult efforts must precede a definition of the precise projects, for it is their results which will form the basis of these studies.

René Ceresuela
Chief of the Research Subdivision
ONERA

REFERENCES

1. Ferry, A. Goals of Hypersonic Aerodynamics. Astronautics and Aeronautics. October 1966.

2. Heldenfels, R.R. Structural Prospects for Hypersonic Air Vehicles. Fifth Congress ICAS, London, September 1966.

3. Becker, John V. Studies of High Lift/drag Ratio Hypersonic Configurations. Fourth Congress ICAS, Paris 1964.

4. Gregory, T.J., L.J. Williams and D.E. Wilcox. The Airbreathing Launch Vehicle for Earth Orbit Shuttle-Performance and Operation. A.I.A.A. Paper 70-270, Cape Canaveral, February 4-6, 1970.

5. Henry, J.R. and C.H. McLellan. The Airbreathing Launch Vehicle for Earth-Orbit Shuttle-New Technology and Development Approach. A.I.A.A. Paper 70-269. A.I.A.A. Advanced Space Transportation Meeting CoCoa Beach, Florida, February 4-6, 1970.

6. Eggers, A.J., R.H. Petersen and N.B. Cohen. Hypersonic Aircraft Technology and Applications. Astronautics and Aeronautics, June 1970.

7. Neuman, Richard D. Special Topics in Hypersonic Flow; Section VII: Development of Analytical Techniques for Generalized Three Dimensional Bodies. AGARD V.K.I. Short Course on Aerodynamic Problems of Hypersonic Aircraft. RHODE ST-GENESE, Belgium, 19-23 January 1970.

8. Monnerie, B. and H. Werlé. Etude de l'écoulement supersonique et hypersonique autour d'une aile élancée en incidence (Study of Supersonic and Hypersonic Flow Around a Slender Wing with Incidence). AGARD Conference Proceeding No. 30, LONDON, May 1968.

9. Ceresuela, R. Aerodynamique d'un avion propulsé à Mach 7 (Aerodynamics of a Propelled Aircraft at Mach 7). Fifth AFITAE on Applied Aerodynamics. POITIERS, September 1968.

10. Grenlesky, S.E. and F.S. Billig. Investigation of an Actively Cooled Leading Edge for Hypersonic Ramjet Engine. Journal of Aircraft. Vol. 5, No. 4, July-August 1968.

11. Hill, M.L. Materials for Small Radius Leading Edges for Hypersonic Vehicles. Journal of Spacecraft, Vol. 5, No. 1, January 1968.

12. Johnston, P.J., J.M. Cubbage and J.P. Weidner. Studies of Engine-Airframe Integration on Hypersonic Aircraft. A.I.A.A. Paper 70-542. TULLAHOMA, May 1970.

13. Wolowicz, C.H. and L.W. Strutz. Preliminary Flight Evaluation of Stability and Control Derivatives and Dynamic Characteristics of the Unaugmented XB 70 A Airplane, Including Comparisons with Predictions. NASA T.N. D. 4578, May 1968.

14. Griffith, B.J. and D.E. Boylan. Reynolds Number and Mach Number Simulation of APOLLO and GEMINI Re-entry; Comparison with Flight. AGARD Conference Proceedings, No. 30, LONDON, May 1968.

15. Ceresuela, R. and J. Coulomb. Theoretical and Experimental Study of the Effectiveness of Control Surfaces in Supersonic Flight. Aer. et Astr. No. 18, 1970-1972, pp. 15-28.

16. Carriere, P. and M. Sirieix. Facteurs d'influence du recollement d'un écoulement supersonique (Factors Influencing Reattachment of Supersonic Flow). Tenth Congress on Applied Mechanics, STRESA, 1960. ONERA Publication No. 102, 1961.

17. Rose, W.C. et al. Interaction of an Oblique Shock Wave with a Turbulent Boundary Layer. AIAA Journal, Vol. 6, No. 9, September 1968, p. 1792.

18. Roshko, A. and G.J. Thomke. Supersonic, Turbulent Boundary-Layer Interaction with a Compression Corner at Very High Reynolds Number. DOUGLAS Paper, No. 10, May 1969, p. 163. WRIGHT-PATTERSON, 7-8 May 1969.

19. Poisson-Quinton, Ph. and R. Ceresuela. Efficacité et échauffement de gouvernes en hypersonique (Effectiveness and Heating of Control Surfaces in Supersonic Flight). Fifth ICAS Congress. LONDON, September 1966.

20. Michel, R. European Work on Hypersonic Flows. Section 1 — Boundary Layers. Prepared for EUROHYP Meeting, COLOGNE, October 15, 1969; ONERA T.P. No. 770, 1969.

Translated for National Aeronautics and Space Administration under Contract No. NASw 2035, by SCITRAN, P.O. Box 5456, Santa Barbara, California, 93108.